

## Surface-functionalization of PDMS for potential micro-bioreactor and embryonic stem cell culture applications

Cite this: *J. Mater. Chem. B*, 2013, **1**, 987

Fatemeh Sarvi,<sup>a</sup> Zhilian Yue,<sup>bc</sup> Kerry Hourigan,<sup>a</sup> Mark C. Thompson<sup>a</sup> and Peggy P. Y. Chan<sup>\*cd</sup>

This study presents a novel and inexpensive method to prepare a disposable micro-bioreactor for stem cell expansion. The micro-bioreactor was fabricated in the form of a fixed bed bioreactor with a microchannel reactor bed. The micro-bioreactor was constructed from polydimethylsiloxane (PDMS), and the microchannel was functionalized to enable cell adhesion and resistance to bovine serum albumin protein adsorption. The PDMS reactor bed surface was activated by oxygen plasma, then aminized with trimethoxysilylpropyl(polyethyleneimine), followed by grafting with carboxymethyl cellulose (CMC) and gelatin in sequence. The functionalized PDMS surface demonstrated improved hydrophilicity and antifouling properties. The grafting of gelatin promoted cell adhesion. The functionalized surface was found to be biocompatible with MDA-MB-231 and Oct4b2 cells and was demonstrated to facilitate cell proliferation. The expanded Oct4b2 cells retained their proliferation potential, undifferentiated phenotype and pluripotency.

Received 24th August 2012  
Accepted 22nd November 2012

DOI: 10.1039/c2tb00019a

[www.rsc.org/MaterialsB](http://www.rsc.org/MaterialsB)

### Introduction

Embryonic stem cells (ESCs) are pluripotent cells with unlimited self-replicating ability; more importantly, they have the potential to differentiate (pluripotency) into all types of cells with different functions both *in vitro* and *in vivo*.<sup>1</sup> ESCs are excellent choices of an *in vitro* cell model for regenerative medicine, functional genomics, human developmental biology and drug discovery study. However, the use of these cells requires a readily available source of stem cells and/or their differentiated derivatives outside a living body, which is a challenge in their cultivation. Unlike many traditional processes that use a cell's capability to produce a protein, the use of stem cells aims to generate the cells themselves as the product. Some of the applications will benefit from the direct expansion of stem cells (for example, hematopoietic stem cell transplantation),<sup>2</sup> whereas others will require the production of a specific differentiated cell type with defined characteristics. This can be done either by controlling the differentiation in a very specific path or by elimination of undesirable cell types that could arise during the production (differentiation) process. The present day exponentially growing effort of stem cell research is having a major need for convergence of more efficient and appropriate laboratory technologies to sustain the growth. One

such technology is the bioreactor system, which can be defined as an industrial form of the contained reaction vessel with well-defined, controlled conditions for specific culture outcomes.<sup>3</sup> Compared with static culture conditions, the use of bioreactors can overcome some limitations of static culture, including the lack of mixing and the need for frequent medium replacement rates.<sup>4</sup> For instance, a recent study has shown that induced pluripotent stem cells can be generated more efficiently in a stirred culture compared to a static culture.<sup>5</sup> However, the success of maximum expansion of stem cells is dependent not only on the bioreactor design but also on several other parameters. It is well known that stem cells can start to differentiate into mature tissue cells and lose their pluripotency when they are exposed to the intrinsic properties of their extracellular matrix (ECM). ECM stimuli, including matrix structure, chemistry, substrate elasticity, and the presence of growth factors, can elicit stem cell differentiation.<sup>6,7</sup> The manipulation of the intrinsic parameters may render these cells unsuitable for various uses, and hence optimization of the extrinsic parameters is a more suitable method for the purpose of getting maximum expansion of stem cells in a bioreactor.

Microfluidic devices expand our ability to control material transport, and material manipulation, at the micro-scale. Microfluidic systems are particularly advantageous for biological and medical applications; these advantages include the ability to create bio-mimetic structures that mimic the *in vivo* cellular microenvironment,<sup>8</sup> allow experimental parallelization under well-controlled conditions, reduce reagent consumption, and require shorter sample analysis time.<sup>9</sup> Micro-bioreactors are the miniaturized versions of conventional bioreactors,

<sup>a</sup>Department of Mechanical and Aerospace Engineering and Division of Biological Engineering, Monash University, Clayton, Australia

<sup>b</sup>Intelligent Polymer Research Institute, University of Wollongong, Australia

<sup>c</sup>School of Applied Science, RMIT University, Australia. E-mail: [peggy.chan@rmit.edu.au](mailto:peggy.chan@rmit.edu.au); Tel: +61 3 9925 2660

<sup>d</sup>Melbourne Centre for Nanofabrication, Australia

where high-throughput cell based assays can be carried out at low cost compared with their macro-scale counter-parts. For the development of a micro-bioreactor for stem cell expansion, the micro-bioreactor should mimic the *in vivo* microenvironment of stem cells in order to retain the self-replicating ability and pluripotency of stem cells. The construction materials for the micro-bioreactor should be carefully chosen avoiding stimuli such as growth factors, but yet they should be biocompatible and should be surface functionalized to provide cell adhesion sites, since pluripotent stem cells are anchorage dependent.<sup>1</sup>

Polydimethylsiloxane (PDMS) is a popular material which has been widely used for microfluidic device construction, especially for biological applications due to its attractive properties, including elastomeric properties that are similar to soft biological tissues, biocompatibility, optical transparency, high gas permeability, ease of fabrication (simple fabrication by replica molding), and cost effectiveness.<sup>10–12</sup> Despite the advantages of PDMS, the major drawbacks of using untreated PDMS are its low cell adhesiveness, high hydrophobicity, which restricts fluid flow in microchannels, and surface fouling problems, resulting in substantial sample loss and low device performance.

The properties of micro-bioreactor surfaces have a strong influence on cell analysis. A micro-bioreactor surface should be able to support cell growth, and should be protein resistant in order to prevent undesired adsorption of analyte molecules such as protein and DNA. The native PDMS surface is not suitable for stem cell cultivation; when using a PDMS based micro-bioreactor, the PDMS surface should be functionalized to prevent protein adsorption, to avoid contamination and to minimize the loss of precious samples that are of micro/nano volume.<sup>13</sup> PDMS surfaces can be functionalized by plasma treatment to create silanol groups. The activated surface is then functionalized with amine groups as anchors for further grafting with a hydrophilic polymer to prevent protein adsorption. (3-Aminopropyl)triethoxysilane (APTES) and (3-aminopropyl)trimethoxysilane (APTMS) are organosilanes that are commonly used to introduce amine groups for further protein or biomolecule immobilization on microfluidic devices.<sup>14</sup>

This study presents a novel and inexpensive method to prepare a disposable micro-bioreactor for stem cell expansion. The micro-bioreactor was constructed using PDMS in the form of a fixed bed reactor with a microchannel serving as the reactor bed. A method to functionalize the micro-bioreactor to facilitate stem cell adhesion and propagation was developed. Herein, trimethoxysilylpropyl(polyethyleneimine) was investigated as an alternative organosilane for micro-bioreactor surface aminization. Trimethoxysilylpropyl(polyethyleneimine) has been shown to aminize PDMS surfaces more efficiently compared with APTMS and *N*-(3-trimethoxysilylpropyl)diethylenetriamine,<sup>15</sup> due to the presence of multiple amines per molecule. Carboxymethyl cellulose (CMC) is a derivative of cellulose that is commonly used as a Food and Drug Administration (FDA)-approved disintegrate in pharmaceutical manufacturing.<sup>16</sup> It is water-soluble, biocompatible and available abundantly at low cost, making it an attractive biomaterials candidate. CMC has been employed as a wound dressing material and a co-excipient with drugs.<sup>17</sup> CMC

has been demonstrated to inhibit postsurgical and postoperative adhesions.<sup>18–20</sup> This study investigated the potential of using CMC as a low-cost non-fouling material. The aminized PDMS microchannel was further functionalized with CMC, and the resulting protein resistance was examined.

Most mammalian cells are anchorage dependent. Cell adhesion is essential for organogenesis, wound healing, tissue homeostasis and remodelling. Cell attachment to a proper anchoring surface also plays an important role in regulating cell survival, cell cycle progression, and tissue-specific phenotype expression. Abnormal adhesion processes can lead to many pathological conditions such as tumour metastatic invasion and blood clotting defects.<sup>21</sup> PDMS and CMC possess many favourable properties that make them attractive as a material for microfluidic device fabrication, but they both lack ligands that mediate cell adhesion.

Gelatin derived from collagen has widely been used for pharmaceutical and medical applications due to its abundant availability, cost-effectiveness, excellent biodegradability and biocompatibility, and non-immunogenic properties.<sup>22</sup> It is known that gelatin contains arginine–glycine–aspartate (RGD) motifs; RGD peptides provide a high-affinity site for cell binding, and are often incorporated in biomaterials to promote cell adhesion.<sup>23,24</sup> Therefore, the CMC functionalized microchannel was further functionalized with gelatin, which contains RGD peptides to promote cell–substrate adhesion. The performance of the bio-functionalized micro-bioreactor was evaluated for its performance in facilitating cell expansion. The ability of the bio-functionalized surface to maintain stem cell pluripotency was also evaluated.

## Experimental

### Materials

PDMS substrates were prepared using a silicon elastomer kit (Sylgard 184, Dow Corning, MI) and mixed at a 1 : 10 curing agent to base ratio. Trimethoxysilylpropyl(polyethyleneimine) (50% in isopropanol) ( $M_w = 2000–4000$ ) was purchased from Gelest Inc, USA. *N*-Hydroxysuccinimide (NHS), 1-ethyl-3-(3-dimethylaminopropyl)carbodiimide hydrochloride (EDC), carboxymethyl cellulose sodium salt (CMC,  $M_w \sim 90$  kDa), albumin–fluorescein isothiocyanate conjugate (BSA–FITC), bovine serum albumin (BSA), acid orange II, and 2-(*N*-morpholino)ethane sulfonic acid (MES) were purchased from Sigma-Aldrich, Australia. Calcein AM, 4',6-diamidino-2-phenylindole, dilactate (DAPI), Texas Red®-X phalloidin, Dulbecco's modified Eagle's medium (DMEM), non-essential amino acids, GlutaMAX™, and penicillin–streptomycin were obtained from Life Technologies, Australia. *n*-Hexane was obtained from Merck. Gelatin ( $M_w = 80–140$  kDa) was obtained from Wako. Unless stated otherwise, all other chemicals were purchased from Sigma-Aldrich, Australia.

### Fabrication of PDMS microchannels

The PDMS microchannel was fabricated using the photolithographic fabrication method. A dark field photomask with a

microchannel pattern of 200  $\mu\text{m}$  width, 50  $\mu\text{m}$  height and 3 cm length was designed using AutoCAD. Standard photolithography was employed to fabricate the Si master mold for PDMS replication. In brief, SU8-2050 (Microchem) was spin coated on a wafer at 500 and 1500 rpm for 5 s and 30 s, respectively. The spun coated wafer was placed on a hotplate at 65  $^{\circ}\text{C}$  and 95  $^{\circ}\text{C}$  in sequence for 5 min and 20 min, respectively. The wafer was then allowed to cool to RT. The photomask was lowered over the photoresist coated wafer to form a sandwich assembly, and was irradiated under UV at 240  $\text{mJ cm}^{-2}$  in a Contact Aligner (Mask Aligner, EVG 620). After UV-irradiation, the wafer was baked at 65  $^{\circ}\text{C}$  for 5 min followed by 95  $^{\circ}\text{C}$  for 10 min and then cooled down to RT. The wafer was subsequently developed for 15 min followed by rinsing in acetone and isopropyl alcohol (IPA) before drying with dry nitrogen. The patterned master mold was placed in a Petri dish.

The PDMS prepolymer was cast onto the silica master mold. After curing at 85  $^{\circ}\text{C}$  for 4 h, the PDMS microchannel replica was gently peeled off from the master mold and cut into a rectangular plate of dimension 2  $\times$  3  $\text{cm}^2$  to prepare micro-bioreactor assemblies. Holes for inlet and outlet ports at both ends of the microchannel were punched with a syringe needle. The PDMS substrates were then washed with hexane for 2 days to remove the uncured prepolymer, followed by isopropanol to remove contaminants.

#### Aminization of PDMS substrates (PDMS-NH<sub>2</sub>)

The PDMS substrate containing the microchannel pattern was activated by oxygen plasma treatment at 1000 mTorr for 60 s in a plasma cleaner (Harrick Plasma, PDC-001/002, USA) to generate silanol groups, and then bound to a microscope slide immediately to allow irreversible sealing (Fig. 1). The microchannel was filled with 4% (v/v) trimethoxysilylpropyl(polyethyleneimine) in acetone in a single injection using a syringe, and allowed to react for 2 h at RT. The modified microchannel was rinsed with ethanol and deionized (DI) water to remove any unbound polymer, and dried at 65  $^{\circ}\text{C}$  for 3 h. The microchannel was then equilibrated with MES buffer (50 mM, pH 5.0) for next step modification. The aminized PDMS substrate is denoted as PDMS-NH<sub>2</sub>.

#### Determination of amine content

The amount of surface accessible amine was quantified using an Acid Orange II assay.<sup>25</sup> In brief, PDMS films were cut into 2  $\times$  2  $\text{cm}^2$  samples and aminized according to the above aminization protocol; samples were incubated in 1 ml of Acid Orange II solution in DI water (500  $\mu\text{M}$ , pH 3) overnight at RT. Unbound Acid Orange II was removed by washing the samples with copious water at pH 3 (adjusted by HCl). The samples were then incubated in 1 ml of DI water at pH 12 (adjusted with NaOH) overnight to allow the bound dye to detach. The amount of the bound dye was quantified by measuring the optical density at 492 nm. Unmodified PDMS substrates served as controls. A series of Acid Orange II standard solutions (100–500  $\mu\text{M}$ ) were prepared in DI water at pH 12 and used to establish the standard curve. The amount of surface amine groups was calculated

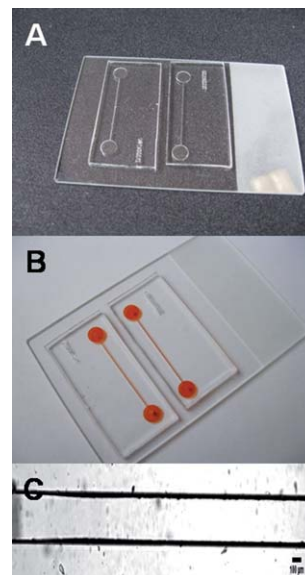


**Fig. 1** Photos of (A) a PDMS micro-bioreactor, (B) a food-dye filled micro-bioreactor device showing inlets, outlets and microchannels, (C) an enlarged bright field view of a microchannel, photo taken under an optical microscope (scale bar = 100  $\mu\text{m}$ ).

based on the assumption that each Acid Orange II molecule complexes with one molecule of the amine.

#### Surface grafting of CMC onto PDMS-NH<sub>2</sub> substrates (PDMS-NH-CMC)

EDC and NHS (1 : 1) were added to 0.6  $\text{mg ml}^{-1}$  CMC in MES buffer (50 mM, pH 5.0) to obtain a final concentration of 2.0  $\text{mg ml}^{-1}$ , and allowed to react for 30 min at RT. The activated CMC solution prepared according to the above procedures was injected into the PDMS-NH<sub>2</sub> microchannel until the microchannel was fully filled, and was allowed to react at RT overnight. The microchannels were then rinsed by injecting MilliQ water to remove residual reagents followed by injecting 0.1 MES buffer. The samples were dried in an oven at 65  $^{\circ}\text{C}$  for 3 h. The CMC grafted substrate is denoted as PDMS-NH-CMC.

#### Surface grafting of gelatin onto PDMS-NH-CMC substrates (PDMS-NH-CMC-GEL)

Conjugation of gelatin on PDMS-NH-CMC was performed under aseptic conditions. PDMS-NH-CMC microchannels were first sterilized in 70% ethanol overnight. One ml of EDC (2.0  $\text{mg ml}^{-1}$ ) and NHS (2.0  $\text{mg ml}^{-1}$ ) in MES buffer (pH 5) was filter sterilized before injecting into a PDMS-NH-CMC microchannel in a single-injection until the microchannel was fully filled. After reacting for 30 min at RT, sterile gelatin solution (300  $\mu\text{g ml}^{-1}$ ) in phosphate buffered saline (PBS) was injected into the activated microchannel in a single-injection until the microchannel was fully filled, and allowed to react overnight at RT. The microchannel was then rinsed by injecting sterile MilliQ water followed by PBS. The gelatin-grafted substrate is denoted as PDMS-NH-CMC-GEL.

### Surface characterization of functionalized PDMS substrates

To characterize the functionalized surfaces, PDMS films were cut into  $2 \times 2 \text{ cm}^2$  samples and functionalized according to the aminization and surface grafting procedures described above. The surface composition analysis of functionalized PDMS was carried out using Fourier Transform Infrared Spectroscopy (FTIR spectrometer, Spectrum 100 series, PerkinElmer, USA). Static water contact angle (WCA) measurements of functionalized PDMS substrates were performed using a sessile drop method ( $2 \mu\text{l}$ , MilliQ water) with an optical contact angle measuring instrument (OCA20, Dataphysics Instruments GmbH, Germany). The measurements were performed on at least three different areas on each substrate and the values were averaged. To assess the stability of surface functionalization, the WCAs of PDMS-NH<sub>2</sub> and PDMS-NH-CMC were monitored over a period of 25 days.

### Protein adsorption

Protein adsorption of functionalized substrates was investigated using a method modified from Goda *et al.*<sup>26</sup> In brief, after being equilibrated in PBS at RT overnight, samples with a defined size ( $4.0 \text{ cm}^2$ ) were immersed in a freshly prepared BSA solution ( $3 \text{ mg ml}^{-1}$ ,  $1 \text{ ml}$  per sample). Adsorptions were allowed to proceed at RT overnight under gentle shaking. The samples were then rinsed with PBS and treated with 1% sodium dodecyl sulphate (SDS) ( $1 \text{ ml}$  per sample) for 20 min to remove the adsorbed protein. The amount of adsorbed protein was quantified using a Micro BCA protein assay kit (Thermo Scientific, Australia). In a separate study, protein adsorption on PDMS and PDMS-NH-CMC was visualized by treating the surface with BSA-FITC using a method modified from Ferrando *et al.*, 2005; Lu *et al.*, 2008; and Wei *et al.*, 2011,<sup>27–29</sup> and the images were acquired using a laser scanning confocal microscope (Nikon A1Rsi MP) with an excitation wavelength of 488 nm and an emission wavelength of 550 nm. The comparison images were obtained using the same confocal microscopy setting.

### Cell culture

MDA-MB-231 (human mammary gland adenocarcinoma) and Oct4b2 (murine-derived embryonic stem cell) cell lines obtained from the Monash Institute of Medical Research (Clayton, VIC, Australia) were employed to investigate cell adhesion and proliferation onto the modified PDMS substrates. MDA-MB-231 cells were maintained in high glucose DMEM (11965, Gibco®) supplemented with 10% fetal bovine serum (FBS), and 1% penicillin-streptomycin at 37 °C in a humidified 5% CO<sub>2</sub> incubator. Oct4b2 cells were maintained in high glucose DMEM (11995, Gibco®) supplemented with 10% FBS (JRH Biosciences, Australia), 1% non-essential amino acids, 1% GlutaMAX™, 0.5% penicillin-streptomycin, 0.1 mM β-mercaptoethanol, and 1000 U ml<sup>-1</sup> ESGRO Leukemia inhibitory factor (LIF, Chemicon, Australia). Prior to cell seeding, all substrates were sterilized in 70% ethanol overnight followed by rinsing with sterile PBS. MDA-MB-231 and Oct4b2 cells were seeded

separately onto PDMS or the functionalized PDMS substrate at densities of  $80 \times 10^3$  and  $40 \times 10^3 \text{ cell cm}^{-2}$ , respectively. Pluripotency of Oct4b2 cells was monitored by examining their GFP expression using X71 Olympus fluorescence microscopes. The cell adhesion and cell growth were examined using optical microscopy and laser scanning confocal microscopy. Cell counting was performed using a hemocytometer after trypsinization. For visualization, the nucleus of cells was stained with DAPI, while the filamentous actin (F-actin) of cells was stained with Texas Red®-X phalloidin. In brief, samples were fixed with 4% formaldehyde for 20 min at RT and washed 3 times with  $1 \times$  PBS buffer, and then permeabilized with 0.1% Triton X-100-PBS for 2 min, and washed with PBS. The samples were further incubated with 1% bovine serum albumin in PBS (BSA-PBS) for 15 min, followed by Texas Red®-X phalloidin ( $1/1000$  in 1% BSA-PBS) staining for 1 hour. DAPI was then added to the samples and incubated for 5 min. Cell counting was also performed to quantify cell adhesion and cell proliferation.

### Statistical analysis

All experiments were performed in at least 3 replicates. The results are presented as average values  $\pm$  standard deviation. Multiple groups of data were statistically analyzed using ANOVA (analysis of variance); two groups of data were statistically analyzed using the unpaired Student's *t*-test, *p* values lower than 0.05 were considered statistically significant.

## Results and discussion

### Surface functionalization

Fig. 2 illustrates the scheme used for microchannel functionalization. Prior to surface functionalization, the PDMS substrates were washed with hexane to remove the uncured monomer, as the migration of low molecular weight species from the bulk to the surface is known as one of the major causes of hydrophobicity recovery of PDMS.<sup>30</sup> Oxygen plasma was employed to treat the PDMS substrate, as plasma treatment has been shown to preferentially remove organic contaminants as well as generate silanol (Si-OH) groups on PDMS.<sup>31</sup> The presence of hydrophilic silanol groups allows microchip sealing and further aminization. It is well known that the effect of plasma treatment is transient as hydrophobic recovery occurs.<sup>31,32</sup> Therefore immediately after plasma treatment, the PDMS substrate was bonded to a microchip to form an irreversible seal, trimethoxysilylpropyl(polyethyleneimine) was then quickly injected into the microchannel to introduce amine groups on the inner surface of the microchannel to form PDMS-NH<sub>2</sub>.

CMC was conjugated onto the PDMS-NH<sub>2</sub> surface *via* EDC-NHS coupling to form a hydrophilic layer preventing non-specific protein adsorption. CMC grafting introduces carboxyl groups on the surface of PDMS-NH<sub>2</sub> to form PDMS-NH-CMC and enables further modification with desired biomolecules. An EDC-based coupling technique was employed as the EDC reagent does not remain as a part of the linkage, which eliminates the possibility of releasing cytotoxic agents when the polymer degrades. In addition the by-product produced by the

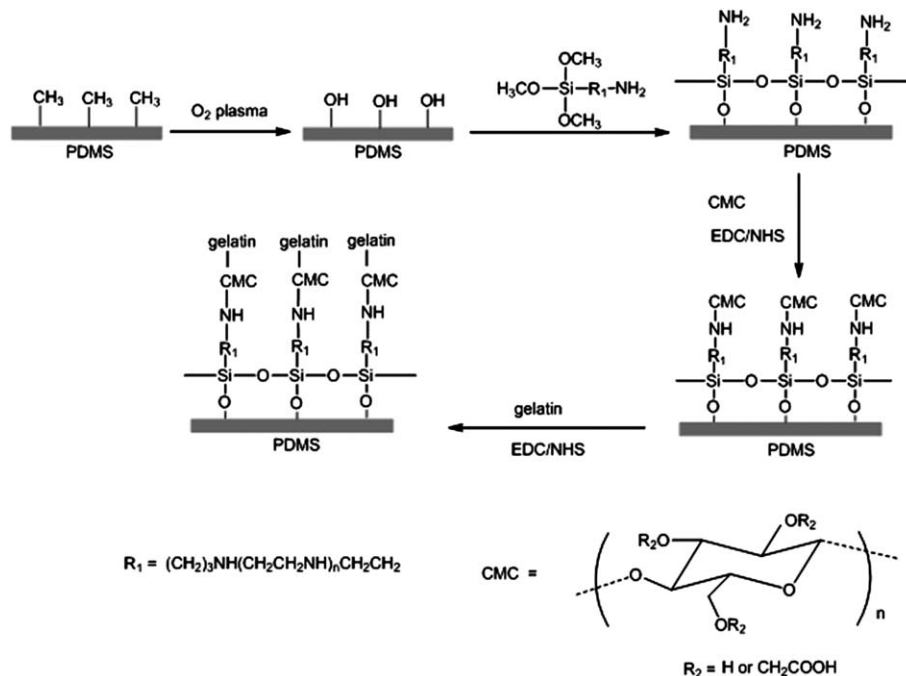


Fig. 2 Schematic illustration of the surface functionalization procedure.

coupling reaction is water-soluble and can be easily removed.<sup>33</sup> Gelatin, as a model biomolecule, was grafted onto PDMS-NH-CMC to form PDMS-NH-CMC-GEL *via* EDC-NHS coupling to promote cell-substrate interactions.

### Physicochemical properties of functionalized PDMS

Acid Orange II assay was performed to confirm and quantify the amount of amine groups introduced on the PDMS substrate. Fig. 3 shows that the amount of amine present on PDMS-NH<sub>2</sub> is significantly higher than that on the non-treated PDMS substrate, indicating that the aminization process was successful.

Fig. 4 reveals the FTIR spectra of PDMS (curve A), PDMS-NH<sub>2</sub> (curve B), PDMS-NH-CMC (curve C), and PDMS-NH-CMC-GEL (curve D) substrates, respectively. It has been shown that

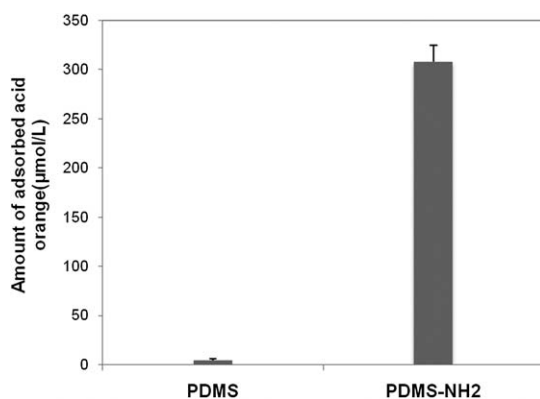


Fig. 3 Quantification of surface amine on native PDMS and PDMS-NH<sub>2</sub> by measuring the amount of adsorbed acid orange.

polyethyleneimine alone has characteristic peaks at 1630 and 1565 cm<sup>-1</sup>.<sup>34</sup> The PDMS-NH<sub>2</sub> spectrum (curve B) showed new bands at 1520–1720 cm<sup>-1</sup> and 3360 cm<sup>-1</sup>, arising from the NH deformation and NH stretching of the amine groups, respectively. The peak at ~1600 cm<sup>-1</sup> on the PDMS-NH-CMC spectrum (curve C) is attributed to the carboxylic acid groups, which confirmed the successful grafting of CMC onto PDMS-NH<sub>2</sub>.

Verification of the existence of successive functionalization of PDMS was obtained through WCA measurements as the functionalization was conducted. Fig. 5A shows the change in wettability of PDMS after each functionalization step. The WCA of native PDMS was found to be 116 ± 0.3°, which is consistent with the inherent hydrophobicity of PDMS. After the PDMS was aminized, the WCA of the resulting PDMS-NH<sub>2</sub> was found to be 55°, and the WCA decreased to 22° after further functionalization with CMC, indicating that the hydrophobic PDMS surface has been converted to a hydrophilic surface. The enhanced

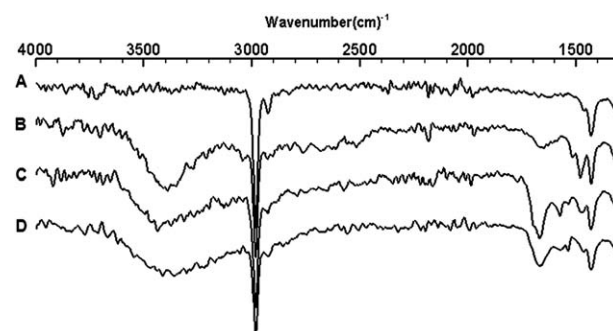
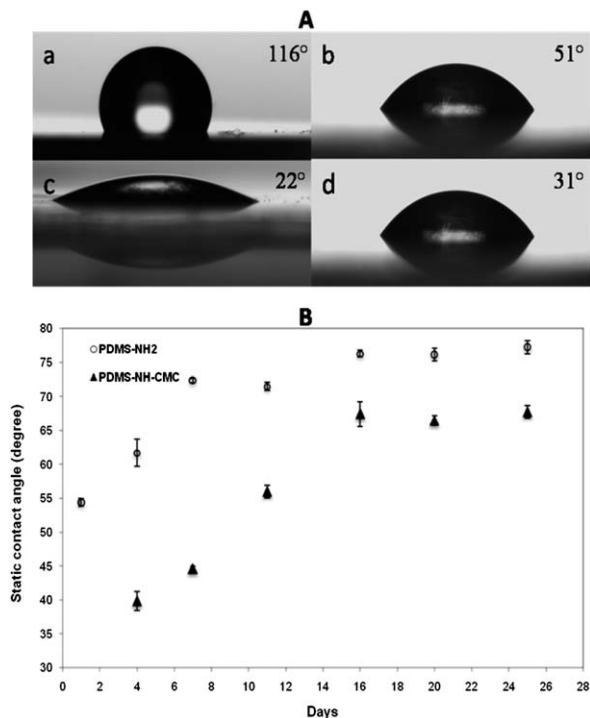


Fig. 4 FTIR spectra of (a) PDMS, (b) PDMS-NH<sub>2</sub>, (c) PDMS-NH-CMC, and (d) PDMS-NH-CMC-GEL.



**Fig. 5** (A) Static water contact angle of (a) PDMS, (b) PDMS-NH<sub>2</sub>, (c) PDMS-NH-CMC, and (d) PDMS-NH-CMC-GEL substrates measured at day 1. (B) shows the variation of static contact angles of PDMS-NH<sub>2</sub> and PDMS-NH-CMC as a function of the storage time in air.

hydrophilicity is attributed to the surface hydroxyl and carboxylic acid groups on PDMS-NH-CMC. Further gelatin conjugation slightly increases the WCA from 22° to 31°, due to the presence of hydrophobic amino acid components on the modified surface. Nevertheless, the final characteristic of functionalized PDMS is still much more hydrophilic than native PDMS.

The WCAs of PDMS-NH<sub>2</sub> and PDMS-NH-CMC were monitored for another 25 days to assess the stability of the surface functionalization. As shown in Fig. 5B, both PDMS-NH<sub>2</sub> and PDMS-NH-CMC substrates remained hydrophilic over a period of 16 days. After that time, the WCAs of PDMS-NH<sub>2</sub> and PDMS-NH-CMC become stabilized at around 67° and 77°, respectively. Although partial recovery of hydrophobicity was observed after 16 days, both PDMS-NH<sub>2</sub> and PDMS-NH-CMC substrates remain more hydrophilic compared to native PDMS that displayed a WCA of 116° (Fig. 5A). It was observed that the WCA of PDMS-NH-CMC was lower than that of PDMS-NH<sub>2</sub> at each time point, indicating that the grafting of CMC onto the PDMS-NH<sub>2</sub> surface further reduces the hydrophobicity.

It is known that hydrophobicity recovery of PDMS is not solely due to migration of low molecular weight species, but also due to physical surface recovery of PDMS, *i.e.*, reorientation of PDMS.<sup>35</sup> The high molecular weight CMC forms a dense hydrophilic coating on the PDMS surface; this coating minimizes the underlying PDMS from air exposure and subsequent PDMS re-orientation, thereby improving surface hydrophilicity retention. The use of a high molecular weight organosilane,

trimethoxysilylpropyl(polyethylene imine), may also contribute to the formation of a dense coating that prevents PDMS surface recovery. In addition, the hydrophobicity recovery of PDMS can also be affected by storage conditions; for example, it is known that storing the samples in a wet environment such as in water and Luria-Bertani broth can retain surface hydrophilicity of PDMS.<sup>36</sup> The storage conditions can be optimized in a future study to maximize the long-term stability of PDMS-NH-CMC hydrophilicity.

### Protein adsorption

BSA is a protein produced by the liver and functions as a transport protein *in vivo*. BSA is the most abundant protein component of bovine plasma.<sup>37</sup> BSA-FITC was selected as a model biofouling protein for the study of protein adsorption on the CMC functionalized substrate, because BSA is inexpensive, well characterized and commonly employed in protein adsorption studies.<sup>38–40</sup> The native PDMS substrate served as the control. As shown in Fig. 6A, BSA-FITC was readily adsorbed by the native PDMS substrate. In contrast, only very weak fluorescent signals were observed for the PDMS-NH-CMC substrate, indicating that the CMC functionalization was effective in preventing BSA adsorption.

The amounts of BSA adsorption on PDMS, PDMS-NH<sub>2</sub>, and PDMS-NH-CMC substrates were quantified using a BCA protein assay. Fig. 6B shows that the amounts of adsorbed BSA decreased significantly in the sequence of PDMS > PDMS-NH<sub>2</sub> > PDMS-NH-CMC.

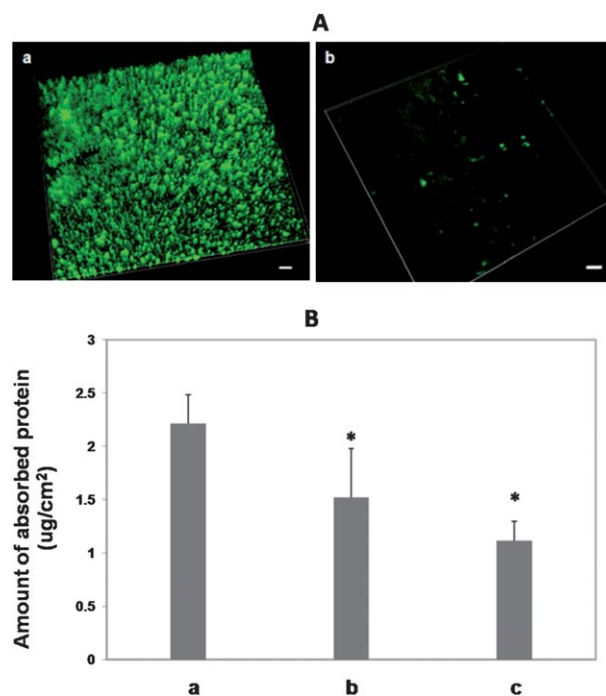


**Fig. 6** (A) Confocal microscopy images showing BSA-FITC adsorption on PDMS and PDMS-NH-CMC (scale bar = 100 μm). (B) shows the influence of surface modification on BSA adsorption on (a) PDMS, (b) PDMS-NH<sub>2</sub>, and (c) PDMS-NH-CMC substrates. Data are presented as average values ± standard deviation (\**p* < 0.05).

Adsorption of BSA on a hydrophobic surface is driven by non-polar attraction between BSA molecules toward the surface. However, adsorption of BSA on a charged surface is predominantly driven by electrostatic interaction between the charged functional groups on BSA molecules and the oppositely charged surface.<sup>41</sup> It is well known that the hydrophobic interaction is the major driving force of protein adsorption, with protein adsorption tending to be greater on a hydrophobic surface compared to a hydrophilic surface.<sup>42</sup> Compared to the native PDMS substrate, the amount of protein adsorbed onto PDMS-NH<sub>2</sub> and PDMS-NH-CMC substrates decreased by about 1.4 and 2 times, respectively. These results suggested that protein adsorption on PDMS is reduced by rendering its surface hydrophilicity through hydrophilic polysaccharide functionalization. At physiological pH, the carboxylic acid groups of CMC are deprotonated and become anionically charged, which is similar to glycosaminoglycans that play major roles as lubricants in cartilaginous tissues.<sup>16</sup> The high water retention and lubricant nature of CMC<sup>43</sup> make it a favourable anti-fouling coating material for PDMS microchannels.

In contrast to carboxylic acid groups, the majority of amine groups of polyethyleneimine are protonated and become cationically charged at physiological pH.<sup>44</sup> The observations of protein adsorption on a surface functionalized with different functional groups by Chapman *et al.*<sup>45</sup> suggest that a reduction in the hydrogen bond donor moieties in the functional group results in a reduction in protein adsorption. Tangpasuthadol *et al.*<sup>46</sup> studied the adsorption of lysozyme (hydroxyl and amine rich protein) and BSA (carboxylic acid rich protein) on a chitosan surface, and found that the adsorption of BSA was lower on carboxylic acid rich chitosan, possibly due to charge repulsion. BSA as a carboxylic acid rich protein was found to adsorb less onto PDMS-NH-CMC substrates compared to PDMS-NH<sub>2</sub> substrates, possibly due to charge-charge repulsion. The result obtained in this study appears to fit well with the study of interaction of charged proteins on hydrophobic and charged hydrophilic surfaces.<sup>42–45</sup>

It was observed that the difference in the protein adsorption level between PDMS and functionalized PDMS obtained by a confocal microscopy method appeared to be greater than that obtained by the BCA protein assay method. The discrepancy may be due to the fact that the confocal microscopy method measures the local protein adsorption, whereas the BCA protein assay method measures the protein adsorption of the whole sample. For future studies, it is suggested that such difference can be expected to be dependent on the chosen measurement method and other factors such as sample homogeneity.

### Cell adhesion

MDA-MB-231 cell adhesion on the PDMS-NH-CMC-GEL substrate was examined and compared to that on PDMS. F-actin was detected using Texas Red®-X phalloidin. F-actin is shown in red while nuclei are shown in blue. As expected, MDA-MB-231 cells appeared to form aggregates and were not attached to the native PDMS substrate. In contrast, cells adhered well onto PDMS-NH-CMC-GEL and proliferated until they reached confluence. Cells adhered onto PDMS-NH-CMC-GEL displayed more well-spread F-actin and normal cell-ECM adhesion (Fig. 7), revealing that the gelatin functionalization process provides appropriate adhesion sites to the cells, thus allowing a normal cytoskeleton formation. For cell growth on the PDMS substrate, the organization of F-actin is more irregular. These results reflect the importance of cell-substrate interaction. They also highlight that cell adhesive ligands can be readily incorporated onto PDMS-NH-CMC to form a PDMS-NH-CMC-GEL based micro-bioreactor while retaining their efficacy for cell adhesion.

### Maintenance of pluripotency and proliferation potential of embryonic stem cells

Oct4b2 cells are undifferentiated murine embryonic stem cells that can be cultured on feeder-free culture medium in the presence of LIF. Oct4b2 cell adhesion and proliferation on the

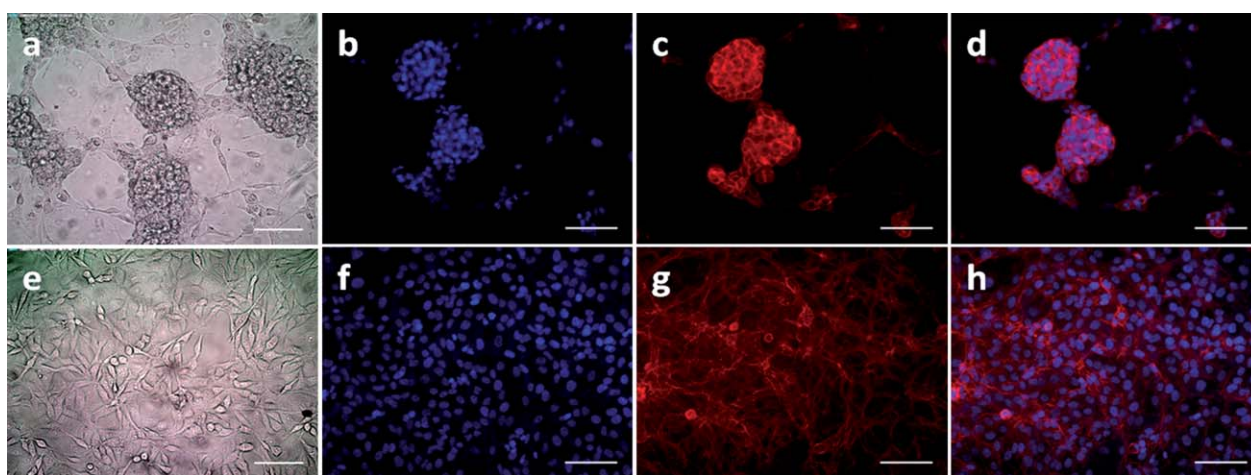


**Fig. 7** Bright field and fluorescence microscopy images of MDA-MB-231 cells cultured on (a–d) PDMS, and (e–h) PDMS-NH-CMC-GEL. (a and e) Bright field images. (b and f) Fluorescence microscopy images show cell nuclei stained by DAPI (blue), (c and g) F-actin stained by Red®-X Phalloidin (red), (d and h) overlay of DAPI and Red®-X Phalloidin fluorescence channels (scale bar = 100 μm).

PDMS–NH–CMC–GEL substrate was monitored and compared to that on PDMS, PDMS–CMC, and a TC treated cell culture dish. The morphology of Octo4b2 cells cultured on different substrates is shown in Fig. 8. As expected, cells cultured on the PDMS substrate were round and small after 1 day, and they appeared to form embryoid body (EB) like structures after 4 days, which were floating in the medium instead of attaching to the PDMS substrate, indicating that the PDMS substrate without any functionalization is not suitable for stem cell adhesion. EB formation entails a transition of ESCs to a three-dimensional structure consisting of three embryonic layers: endoderm, mesoderm and ectoderm lineages, similar to embryogenesis.<sup>47</sup> Unlike anchorage dependent stem cells, EB formation takes place on a non-adherent surface. A hydrophobic PDMS surface is known to promote the development of EBs; the results presented here are consistent with the findings of Valamehr *et al.*<sup>48</sup>

Although, some cell adhesion and cell growth were observed on the PDMS–NH–CMC surface, the cells appeared to be small and not well spread after 1 day, and the cells tend to form aggregates as they proliferated. The aggregation of cells on PDMS–NH–CMC led to a decline in the proliferation rate compared to that of the PDMS–NH–CMC–GEL culture, indicating that the cells did not adhere well onto the PDMS–NH–

CMC substrate due to the lack of cell adhesion ligands. In contrast, cells grown on PDMS–NH–CMC–GEL appeared to be larger with more spatially dispersed bodies. The cell number increased after 4 days similar to those grown on a TC treated cell culture dish. The cell density of PDMS–NH–CMC–GEL was approximately three times higher than that of PDMS–NH–CMC. This indicates that PDMS–NH–CMC–GEL facilitates cell adhesion *via* the RGD peptide moiety on gelatin. Oct4b2 cells contain the Oct4-green fluorescence protein (Oct4-GFP) reporter.

Oct4 is a pluripotency- and germ-cell-specific marker, and the expression of Oct4-GFP is correlated with pluripotency. The pluripotency of Oct4b2 was monitored by examining the green fluorescence protein (GFP) expression of Oct4b2 cells. The maintenance of pluripotency was illustrated through the fluorescence expressed by Oct4-GFP (depicted in green) in the cytoplasm of Oct4b2 cells observed in the fluorescence microscopy images taken 4 days after cell seeding (Fig. 8). The polysaccharide functionalized PDMS, namely PDMS–NH–CMC–GEL, does not appear to cause undesired differentiation of Oct4b2 cells.

### Cell growth in micro-bioreactors

Microfluidic systems have the potential to perform multiple biochemical assays in a single microchip,<sup>9</sup> and provide a

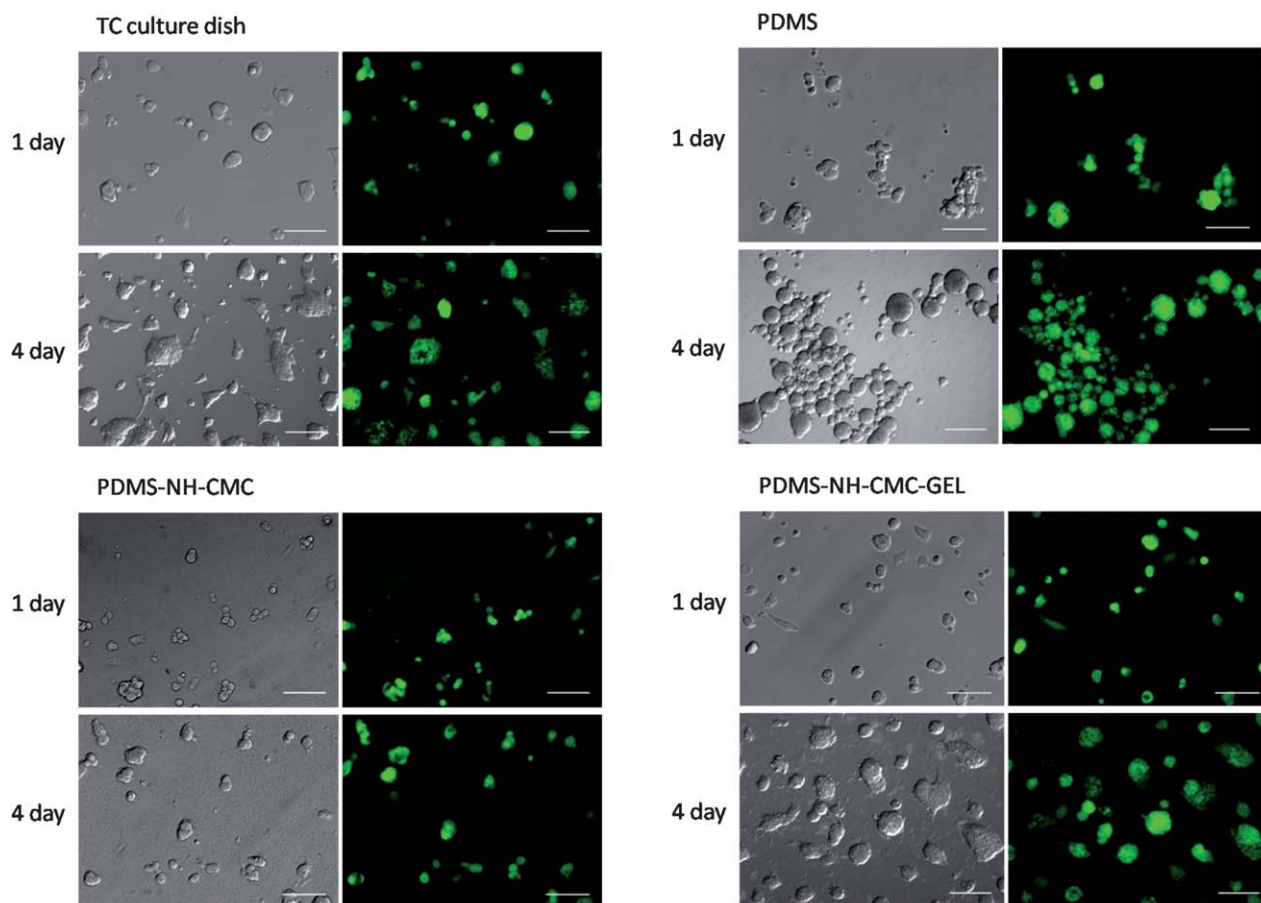


**Fig. 8** Phase contrast images of Oct4b2 cells cultured on different substrates. Fluorescence microscopy images show GFP expression of Oct4b2 cells (scale bar for day 1 is 100  $\mu\text{m}$  and for day 4 is 250  $\mu\text{m}$ ).

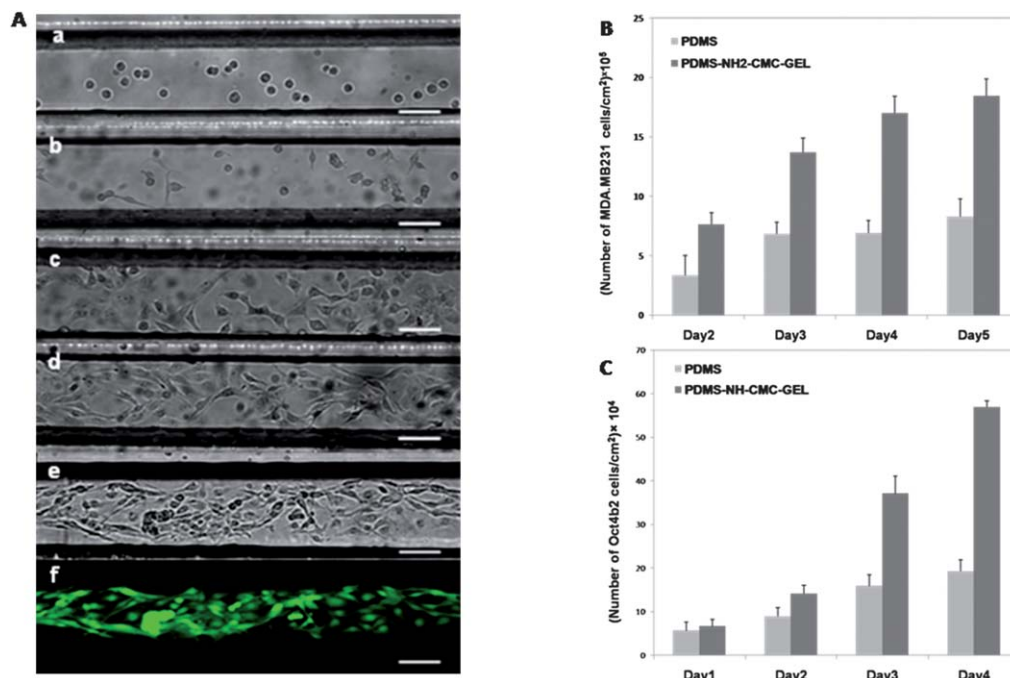


**Fig. 9** (A) Phase contrast images of MDA-MB-231 cells cultured in PDMS-NH-CMC-GEL functionalized microchannels after (a) 0 h, (b) 4 h, (c) 1 day, (d) 3 days, and (e) 4 days after cell seeding. (f) Fluorescence microscopy image of live cells stained by Calcein AM (green) after 4 days (scale bar = 100  $\mu$ m). (B) shows the proliferation of MDA-MB-231 cells, and (C) Oct4b2 cells on PDMS and PDMS-NH-CMC-GEL substrates were monitored over a period of four days.

feasible alternative to the conventional TC cell culture flask by lowering reagent consumption, improving sensitivity and allowing high throughput operation.<sup>49</sup> To show that PDMS-NH-CMC-GEL microchannels can support cell growth, cells were cultured inside the microchannels and monitored over a period of 4 days.

MDA-MB-231 cell attachment and cell morphology were inspected using phase contrast microscopy as shown in Fig. 9A. Four hours after cell seeding, MDA-MB-231 cells appeared to adhere onto the PDMS-NH-CMC-GEL microchannel surface. MDA-MB-231 cells appeared to spread out showing an epithelial-like morphology and proliferating after 1 day. Live/dead staining was performed using Calcein AM to confirm the viability of cells inside microchannels after 4 days. Fig. 9A revealed that the majority of cells remained viable (stained in green) inside the microchannel and demonstrated the ability of the present method to support cell cultivation.

The proliferation of cells on different substrates was quantified and the results are summarized in Fig. 9B and C. The cell growth on the PDMS-NH-CMC-GEL substrate was compared to that on the PDMS control substrate over four consecutive days. The results revealed that the number of cells grown on the PDMS-NH-CMC-GEL substrate was much higher than that cultured on the PDMS substrate, for instance, the number of MDA-MB-231 and Oct4b2 cells on PDMS-NH-CMC-GEL is approximately 2 times and 2.3 times greater than that on PDMS at day three, respectively. The rate of cell proliferation on PDMS-NH-CMC-GEL also appeared to be higher than that on the PDMS substrate. The proliferation of cells implies that the functionalized microchannel surface is biocompatible with cells. It is worth mentioning that the functionalized

microchannel system derived in this study can be employed as a perfusion micro-bioreactor when integrated with an appropriate flow control system. The effects of shear stress on stem cells growth and differentiation compared with those in the static culture are currently under investigation.

## Conclusions

We have developed a novel method to prepare a micro-bioreactor for stem cell expansion. This method is cost effective, and allows functionalization to be carried out by needle injection of reagents into the micro-bioreactor surface, and is thereby compatible with standard microfabrication processes. Enhanced and extended surface hydrophilicity were permitted by the proposed functionalization method. The cytocompatibility has also been demonstrated by cultivating MDA-MB-231 on a functionalized micro-bioreactor surface. We also demonstrated that the functionalized surface facilitates Oct4b2 cell propagation, as well as retaining the undifferentiated phenotype and pluripotency of the cells. The results demonstrate the potential use of the micro-bioreactor as a stem cell study tool.

## Acknowledgements

We acknowledge the funding provided by the Department of Mechanical and Aerospace Engineering at Monash University. Funding for this research was also partly provided through an Australia Research Council Discovery Project Grant ARC DP 120102570 and through the Australia-India Strategic Research Fund BF050038. We also thank Dr Paul Verma from Monash Institute of Medical Research (MIMR) for supplying Oct4b2

cells. We would like to thank Dr Ricky Tjeung for his assistance with microchannel fabrication and Ms Karla Contreras for her assistance with cell culturing. This work was performed in part at the Melbourne Centre for Nanofabrication, an initiative partly funded by the Commonwealth of Australia and the Victorian Government.

## Notes and references

- N. Xu, T. Papagiannakopoulos, G. Pan, J. A. Thomson and K. S. Kosik, *Cell*, 2009, **137**, 647–658.
- Z. Du, H. Cai, Z. Ye and W.-S. Tan, *J. Biotechnol.*, 2012, **164**, 211–219.
- C. A. V. Rodrigues, T. G. Fernandes, M. M. Diogo, C. L. da Silva and J. M. S. Cabral, *Biotechnol. Adv.*, 2011, **29**, 815–829.
- T. Liu, *Comprehensive Biotechnology*, 2nd edn, 2011, vol. 5, pp. 389–396.
- J. Chen and D. Pei, *Nat. Methods*, 2012, **9**, 449–451.
- G. C. Reilly and A. J. Engler, *J. Biomech.*, 2010, **43**, 55–62.
- A. J. Engler, S. Sen, H. L. Sweeney and D. E. Discher, *Cell*, 2006, **126**, 677–689.
- E. Cimetta, E. Figallo, C. Cannizzaro, N. Elvassore and G. Vunjak-Novakovic, *Methods*, 2009, **47**, 81–89.
- L. Y. Yeo, H.-C. Chang, P. P. Y. Chan and J. R. Friend, *Small*, 2011, **7**, 12–48.
- V. Compan, A. Lopez-Aleman, E. Riande and M. F. Refojo, *Biomaterials*, 2004, **25**, 359–365.
- F. Abbasi, H. Mirzadeh and A. A. Katbab, *Polym. Int.*, 2001, **50**, 1279–1287.
- M. L. van Poll, F. Zhou, M. Ramstedt, L. Hu and W. T. S. Huck, *Angew. Chem., Int. Ed.*, 2007, **46**, 6634–6637.
- H. Yan, B. Zhang and H. Wu, *Electrophoresis*, 2008, **29**, 1775–1786.
- N. R. Glass, R. Tjeung, P. Chan, L. Y. Yeo and J. R. Friend, *Biomicrofluidics*, 2011, **5**, 36501–365017.
- Z. Yue, X. Liu, P. J. Molino and G. G. Wallace, *Biomaterials*, 2011, **32**, 4714–4724.
- A. T. Reza and S. B. Nicoll, *Acta Biomater.*, 2010, **6**, 179–186.
- N. A. Ramli and T. W. Wong, *Int. J. Pharm.*, 2011, **403**, 73–82.
- C. K. Ryan and H. C. Sax, *Am. J. Surg.*, 1995, **169**, 154–160.
- J. Ma, Y. Xu, B. Fan and B. Liang, *Eur. Polym. J.*, 2007, **43**, 2221–2228.
- M. A. Lalountas, K. D. Ballas, C. Skouras, C. Asteriou, T. Kontoulis, D. Pissas, A. Triantafyllou and A. K. Sakantamis, *Am. J. Surg.*, 2010, **200**, 118–123.
- A. J. Garcia and D. Boettiger, *Biomaterials*, 1999, **20**, 2427–2433.
- S. Young, M. Wong, Y. Tabata and A. G. Mikos, *J. Control. Release*, 2005, **109**, 256–274.
- H. Shin, S. Jo and A. G. Mikos, *Biomaterials*, 2003, **24**, 4353–4364.
- L. S. Wang, J. E. Chung, P. P. Y. Chan and M. Kurisawa, *Biomaterials*, 2010, **31**, 1148–1157.
- W. Albrecht, B. Seifert, T. Weigel, M. Schossig, A. Hollander, T. Groth and R. Hilke, *Macromol. Chem. Phys.*, 2003, **204**, 510–521.
- T. Goda, T. Konno, M. Takai, T. Moro and K. Ishihara, *Biomaterials*, 2006, **27**, 5151–5160.
- M. Ferrando, A. Rozek, M. Zator, F. Lopez and C. Guell, *J. Membr. Sci.*, 2005, **250**, 283–293.
- T. Lu, X. Chen, Q. Shi, Y. Wang, P. Zhang and X. Jing, *Acta Biomater.*, 2008, **4**, 1770–1777.
- J. Wei, L. Yan, X. Hu, X. Chen, Y. Huang and X. Jing, *Colloids Surf., B*, 2011, **83**, 220–228.
- S. Hemmilä, J. V. Cauich-Rodríguez, J. Kreutzer and P. Kallio, *Appl. Surf. Sci.*, 2012, **258**, 9864–9875.
- M. Farrell and S. Beaudoin, *Colloids Surf., B*, 2010, **81**, 468–475.
- H. T. Kim and O. C. Jeong, *Microelectron. Eng.*, 2011, **88**, 2281–2285.
- P. F. Gratzer and J. M. Lee, *J. Biomed. Mater. Res.*, 2001, **58**, 172–179.
- L. Bertilsson, H. Elwing, B. Liedberg, O. Larm, J. Risinfeld and E. Scholander, *Macromol. Eng.*, 1991, **1**, 49–57.
- D. Bodas and C. Khan-Malek, *Sens. Actuators, B*, 2007, **123**, 368–373.
- L. H. Zhao, J. Lee and P. N. Sen, *Sens. Actuators, A*, 2012, **181**, 33–42.
- T. Mogues, J. Z. Li, J. Coburn and D. J. Kuter, *J. Immunol. Methods*, 2005, **300**, 1–11.
- S. M. Moghimi, *Biochim. Biophys. Acta, Mol. Cell Res.*, 2002, **1590**, 131–139.
- J. Hu, S. J. Li and B. L. Liu, *Biochem. Eng. J.*, 2005, **23**, 259–263.
- Y. L. Jeyachandran, J. A. Mielczarski, E. Mielczarski and B. Rai, *J. Colloid Interface Sci.*, 2010, **341**, 136–142.
- Y. L. Jeyachandran, E. Mielczarski, B. Rai and J. A. Mielczarski, *Langmuir*, 2009, **25**, 11614–11620.
- J. Y. Yoon, H. Y. Park, J. H. Kim and W. S. Kim, *J. Colloid Interface Sci.*, 1996, **177**, 613–620.
- C. Chang and L. Zhang, *Carbohydr. Polym.*, 2011, **84**, 40–53.
- J. D. Ziebarth and Y. Wang, *Biomacromolecules*, 2010, **11**, 29–38.
- R. G. Chapman, E. Ostuni, S. Takayama, R. E. Holmlin, L. Yan and G. M. Whitesides, *J. Am. Chem. Soc.*, 2000, **122**, 8303–8304.
- V. Tangpasuthadol, N. Pongchaisirikul and V. P. Hoven, *Carbohydr. Res.*, 2003, **338**, 937–942.
- H. Kurosawa, *J. Biosci. Bioeng.*, 2007, **103**, 389–398.
- B. Valamehr, S. J. Jonas, J. Polleux, R. Qiao, S. Guo, E. H. Gschwend, B. Stiles, K. Kam, T.-J. M. Luo, O. N. Witte, X. Liu, B. Dunn and H. Wu, *Proc. Natl. Acad. Sci. U. S. A.*, 2008, **105**, 14459–14464.
- I. Meyvantsson and D. J. Beebe, *Annu. Rev. Anal. Chem.*, 2008, **423–449**.